ELSEVIER

Powder Technology 97 (1998) 237–245

POWDER TECHNOLOGY

The tensile strength of cohesive powders and its relationship to consolidation, free volume and cohesivity [1]

José Manuel Valverde [a,*], Antonio Ramos [a], Antonio Castellanos [a], P. Keith Watson [b]

[a] *Dpto. de Electronica y Electromagnetismo, Universidad de Sevilla, 41012 Seville, Spain*

[b] *Xerox, Wilson Research Center, Webster, NY 14580, USA*

Received 20 November 1996; received in revised form 9 February 1998; accepted 18 February 1998

Abstract

The tensile strength of a powder is related to the interparticle force and to the free volume, which, in turn, are related to consolidation stress. The relationship between stress and free volume is described by the state diagram that has been measured at zero shear for a set of cohesive powders (xerographic toners) with a range of concentrations of a flow control additive. The toners are 12.7 μm diameter particles of styrene/butadiene copolymer, and the surface additive is a submicron fumed silica that is used to control the interparticle forces. To overcome problems of sample non-uniformity, powder samples are initially fluidized and then allowed to settle under gravity. The tensile strengths, σ_t, of these powders have been measured by means of a powder bed technique in which gas flow through the bed is increased until the bed fractures due to the tensile stress produced by the gas flow. The overpressure required to fracture the bed then provides a measure of σ_t. The consolidation stress in the bed, σ_c, can be altered by varying the weight of the powder per unit area. Tensile strength is found to be linearly related to the consolidation stress in the limited range of stresses we have investigated, and the slope of this relationship is the same for all additive concentrations below 0.1%; above this concentration the slope decreases, consistent with a change from polymer-dominated to silica-dominated contacts between the particles. From the ratio σ_t/σ_c, we show that the contacts are fully plastic even at zero load, and that hardness of the contacts increases with increasing additive concentration. © 1998 Elsevier Science S.A. All rights reserved.

Keywords: Tensile strength; Cohesive powder; Interparticle force; Free volume; Consolidation stress

1. Introduction

Granular materials can display a complex range of dynamic behavior that, in some senses, parallels the behavior of solids, liquids and gases [1], and this behavior is determined by the interaction of the constituent particles. It is this diversity that makes highly cohesive, fine powders difficult to characterize, and it is for this reason that we have used the state diagram [2] relating consolidation stress, yield stress and free volume, as a means of describing these materials. In particular we have studied powders in the plastic state and the fluidized state.

We have made use of the transition from the fluidized state to the plastic state to initialize the powder and have then used a gas flow through the powder to apply a tensile stress, in order to measure the tensile strength of the powder. The condition under which fluidization occurs depends on the composition of the particles and their size distribution. Geldart [3] proposed a classification of the fluidization behavior of granular materials, based on particle size and density, designated as types A, B, C and D: Type A particles are of low cohesion, and are intermediate in size between categories B and C; these materials are readily fluidized, and appreciable bed expansion occurs before bubbling. Type B particles fluidize readily, but bubbles form at or slightly above the fluidizing velocity; bed expansion is small, with rapid collapse when gas flow ceases (this group includes sand-like materials). Type C materials consist of small, very cohesive particles. These materials cannot usually be fluidized in the conventional sense; they form channels, or lift as a plug in the bed. It is with particles in this size category with which we are concerned.

We have concentrated on polymer particles (xerographic toners) with a volume average size of 12.7 μm diameter, so particle density and size remain constant throughout these experiments. These toners exhibit Type A or C behavior depending on the cohesivity of the material, and we are able to control this by the addition of a flow conditioner (fumed

* Corresponding author. Departamento de Electrónica y Electromagnetismo, Facultad de Física, Avda. Reina Mercedes s/n, 41012 Sevilla, Spain.

[1] Formerly the zero shear state diagram for cohesive powders at low consolidation stresses.

0032-5910/98/$19.00 © 1998 Elsevier Science S.A. All rights reserved.
PII S0032-5910(98)00025-4

silica particles of 7 nm diameter and aggregates of these particles), which reduces the cohesion between grains. Toners with low additives concentration exhibits Type C behavior, but as the additives concentration increases, there is a shift to Type A behavior, although particle size would lead one to predict Type C behavior. For comparison, we have also studied Canon CLC-500 cyan toner, which flows very well and is an ideal Type A material in behavior in spite of its small particle size (8.5 μm volume average diameter).

In analyzing the behavior of these powders, we follow the continuum mechanics approach. It is assumed that there exists a limiting stress function such that stresses lower than those specified by this function cause no deformation, whereas stresses greater than or equal to the limiting stresses cause either yield, with decreasing bulk density, or consolidation, with increasing bulk density. Defining the shear stress τ, the normal pressure σ, and using the (σ,τ) system of coordinates, the critical stresses for a given free volume are depicted in Fig. 1a. Free volume (or void fraction) is defined as $\varepsilon=(1-\rho/\rho_p)$ where ρ is the density of the powder for a given consolidation, and ρ_p is the particle density.

The part of the limiting stress function associated with yield is accompanied by a decrease of bulk density, and is called the yield locus; that part of the limiting function associated with an increase of bulk density is called the consolidation locus. The intersection of the yield locus and consolidation locus defines the critical state (point E in Fig. 1a). The intersection of the yield locus with the σ axis is the tensile strength, σ_t, and the intersection of the consolidation locus with the consolidation stress σ_c. Stresses greater than the consolidation locus cause the powder to consolidate (move to a state of lower ε), and thus move to a higher yield locus corresponding to a lower value of free volume, as shown in Fig. 1b. The porosity ε can be regarded as an independent variable and the generalized yield locus of the powder, referred to as the state diagram, or the condition diagram [2], is a surface in three-dimensional space, σ, τ, ε. As shown experimentally, this surface is also a function of time during which the consolidation is acting, due to the plastic flow of the interparticle contacts.

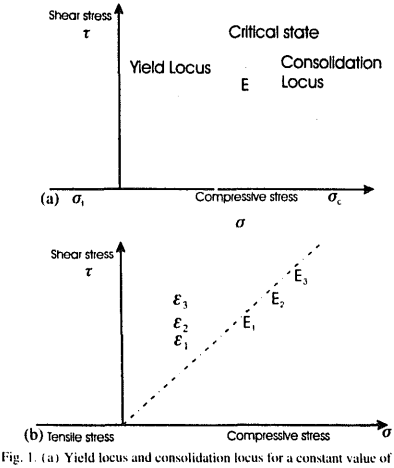

Fig. 1. (a) Yield locus and consolidation locus for a constant value of void fraction, ε. (b) Yield locus and consolidation loci for three values of the void fraction ($\varepsilon_1>\varepsilon_2>\varepsilon_3$).

In this paper, we are concerned with determining the intersection of the state diagram with plane $\tau=0$, i.e., when there is zero shear stress (see Fig. 2). The curve showing the relationship between consolidation stress σ_c and void fraction, ε, is referred to as the consolidation locus for zero shear. In anticipation of our results, the two consolidation loci shown in Fig. 2 correspond to two levels of flow control additive. For a given stress level, particles with high additive concentration are able to rearrange into a more compact state than would be the case for a lower concentration of additive. Once we have a given consolidation, if we now submit the powder to a negative, normal stress, we reach a point at which the powder breaks in tension. The stress at which the powder yields is called the tensile strength, σ_t. An important question then arises as to whether there is a relationship between the compressive stress, which was used to consolidate the powder, and the tensile strength; if the particle contacts behave elastically, we expect σ_t to be relatively independent of σ_c, whereas in the case of plastic deformation of the contacts, there should be a marked increase in σ_t with σ_c.

We have carried out an extensive series of measurements on the cohesive properties of a series of experimental xerographic toners as a function of the initial consolidation stress; the properties measured are the average void fraction and the tensile strength. We are especially interested in low consolidation states as these correspond to conditions of powder

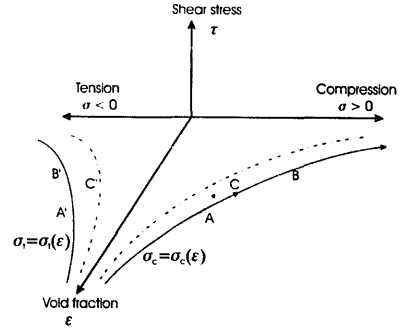

Fig. 2. State diagram for zero shear. A > B Increasing σ, decreasing ε (constant additive concentration). A > C Increasing additive, decreasing ε (ε constant). A', B', C' are values of the tensile strength loci corresponding to consolidation conditions A, B, C respectively.

flow. We find that, for the limited range of consolidation stresses we have examined, there is a linear relationship between tensile strength and consolidation stress; there is also a range of concentrations of flow-control additive for which the proportionality between σ_t and σ_c changes. This proportionality is determined by the kind of contacts that predominate in the powder: that is, polymer–polymer contacts at low additive concentration; silica–polymer contacts at intermediate concentrations; and silica–silica contacts at high additive concentrations.

2. Experimental

Several problems occur when studying the mechanical properties of powders in very low consolidation states: The stresses are very low (a few Pascal) and therefore hard to measure; it is difficult to 'get a grip' on the powder and thus measure its tensile strength; also, uniform powders are hard to create, as a typical powder contains regions of varying degrees of consolidation, so one needs a method of initializing the powder to produce a uniform, reproducible state. To overcome these problems, we have developed a powder bed technique, similar to that described by Rietema [1] and by Tsinontides and Jackson [4], in which gas flow through the powder bed is used to create a tensile stress in the material. In similar approaches, Kono et al. [5] have measured the fracture strength of powders by using the minimum bubbling point in the fluidized bed as the criterion for the fracture of the powder structure, and Seville and Clift [6] have used an inverted bed in which gas flow is reduced until particles 'rain down' from the levitated bed.

In all our measurements, we begin by initializing the sample, which we do by fluidizing the powder and then allowing it to collapse under gravity. The fluidized powder is quite uniform, and when the fluidizing gas is turned off and the bed collapses, a very reproducible, stratified consolidation of the powder is obtained. Fluidized beds are widely used in Chemical Engineering and there is an extensive literature on the subject. However, such work is generally concerned with beds of granular materials of about 50 μm diameter and above, and with relatively close packing; in contrast, our concern is with beds of particles of 12.7 μm diameter, in very open structures that approach the ballistic aggregation limit [7]. One noteworthy observation is that although these materials belong to a size category that is usually described as very difficult to fluidize, we have been able to fluidize them readily. The resolution of this paradox lies in the control of interparticle forces by the use of submicron additives of fumed silica (these are sometimes referred to as flow control additives), to be described in Section 3.

The layout of our powder bed apparatus is shown schematically in Fig. 3. Many of the measurements have been taken using a cylindrical bed of 5.08 cm diameter, with a filter of small enough pore size to ensure that toner particles do not penetrate into the pores, and that the gas stream is

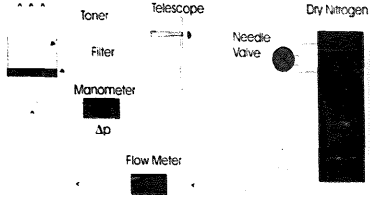

Fig. 3. The fluidized bed apparatus used in these experiments.

distributed uniformly over the lower boundary of the bed (the nominal pore size is 10 to 15 μm, but the effective pore size is smaller). The pressure drop across the filter is measured before and after a test run, and this is used to check that particles have not entered the filter pores and altered the flow impedance. The vertical tube above the bed is approximately 50 cm long and closed at the top by a cellulose paper filter to catch particles suspended in the fluidizing gas. Dry nitrogen is supplied from tanks of compressed gas, and a mass flow controller is used to adjust the flow in the range 0–100 cc/min. The gas flow to the bed is monitored and the pressure drop across the bed plus the filter is measured by a differential pressure transducer in the range of zero to 2300 Pa.

In the case of highly cohesive powders, such as toners with very low additive concentration, in order to initialize the sample, it is necessary to vibrate the bed in order to break up channels that form; these channels conduct the gas away from the bulk of the powder and prevent fluidization (the effect of vibration on the fluidization of cohesive powders is discussed by Marring et al. [8]). Once the fluidizing gas is turned off and the particles are allowed to settle, a very reproducible, stratified consolidation of the powder is obtained. The height of the bed is then measured optically, and from this measurement, together with the particle density, we can compute the average solid fraction, f, given by:

$$f=(1-\varepsilon)=\frac{m}{\rho_p A h} \quad (1)$$

where ε is the average void fraction, m is the mass of the sample, ρ_p the particle density, A the area of the filter, and h the height of the bed. In Fig. 4, the data obtained for the Canon CLC-500 cyan toner are shown. The effect of the compressibility on the packing is clearly seen in the increase of f with h. The reason for the compressibility is that, with increasing compressive stress (due to the weight of the powder), the particles rearrange into a more compact ensemble in the lower levels of the bed. Thus, we observe a decrease of the average void fraction as powder is added to the bed, and the powder undergoes consolidation to a new state. Because of this, we think it reasonable to assume that when the powder settles, the stresses in the bed are on the consolidation locus for zero shear.

A possible complication in the calculation of compressive stress is the influence of the wall effect [9], that is, the

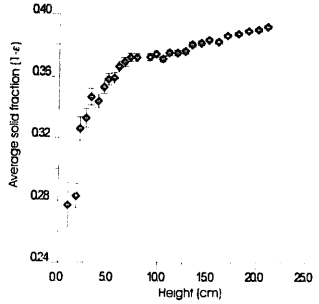

Fig. 4. Variation of the average solid fraction $(1-\varepsilon)$ with height for Canon CLC-500, cyan toner. Diameter of bed = 5.08 cm.

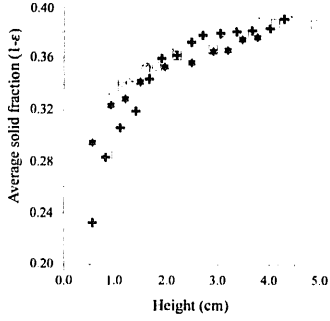

Fig. 5. Average solid fraction as a function of the height for toner with 0.4% additive obtained with different bed diameters: *, 4.09 cm; ○, 4.72 cm; ×, 5.08 cm; +, 8.0 cm; □, rectangular bed.

component of wall friction that is communicated to the bulk of the powder and compensates for part of the downward force. We have studied this by using beds of two different diameters (8.44 and 5.08 cm) for the Canon CLC-500 toner, and we observe that the results are indistinguishable within experimental scatter. We have also checked this with one of the xerographic toners (that with 0.4% silica additive) in beds of diameters: 4.09, 4.72, 5.17, and 8.00 cm, and in a bed of rectangular cross-section 3.35×7.50 cm^2. The results are shown in Fig. 5. We conclude that the wall effect is negligible, at least up to 6 cm bed height. Thus, the consolidation stress at the bottom of the bed is the total weight of the sample per unit area. The next step in the measurement is to submit the layer of powder to an upward-directed flow of gas (dry nitrogen is used to avoid the effect of moisture on the interparticle contacts). When gas flows through a fixed bed of particles, there is a pressure drop across the bed. At low Reynolds numbers, the gas flow is laminar and the pressure drop is a linear function of gas flow rate. The relationship is known as the Carman–Kozeny equation [9]

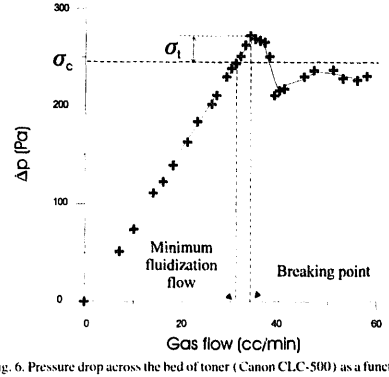

Fig. 6. Pressure drop across the bed of toner (Canon CLC-500) as a function of the gas flow. Total mass, 141.57 g; area of the bed, 20.27 cm^2. The point at which the pressure drop equals the weight of the sample is called the incipient fluidization point. The break point determines the beginning of the expansion.

$$\frac{\Delta p}{h}=C\frac{\mu}{d_p^2}\frac{(1-\varepsilon)^2}{\varepsilon^3}\frac{\phi}{A} \qquad (2)$$

where μ is the dynamic viscosity of the gas, d_p is the particle diameter, ϕ is the gas flow rate, A is the area of the bed, h is the height of the bed, and C is a constant. Values of C of about 180 are reported for relatively large, spherical particles [7]. We obtain the pressure drop across the bed by measuring the total pressure for each flow rate and subtracting the pressure drop across the filter (which is calibrated before and after each test). The result is shown in Fig. 6 for the Canon CLC-500 toner. We see that the pressure drop and, hence the drag force exerted on the particles, increases linearly with the flow rate for the static bed. The value of C in Carman's equation, measured for the Canon CLC-500 toner for different degrees of consolidation, ranges from 200 to 300. Apparently the smaller diameter of Canon CLC-500 toner particles, their very open packing, and their irregular shape causes the pressure drop to grow faster than it would for large, spherical particles. The point at which the pressure drop balances the weight of the powder is referred by some authors as the point of incipient fluidization [1], and by others as the minimum fluidization flow, and represents the point of neutral buoyancy in the bed. If the gas velocity is further increased, the pressure drop continues to increase until interparticle forces are overcome, at which point a sudden decrease in the pressure drop is observed, and this drop coincides with a visible fracture in the bed. Thus, the overpressure (i.e., the overshoot of the pressure drop beyond the weight of the bed) allows us to measure the tensile stress at which the powder yields. As will be shown, this stress does not vary with bed diameter, so we can ignore wall effects, and hence we identify this overpressure with the tensile strength of powder. The fracture of the bed always starts at its lowest point, the bottom of the bed;

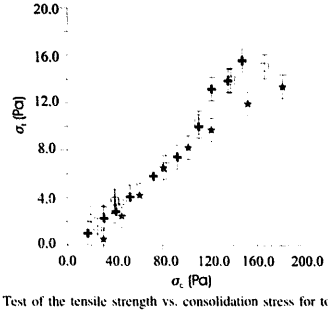

Fig. 7. Test of the tensile strength vs. consolidation stress for toner with 0.4% additive. Bed diameters: +, 4.09 cm; ○, 4.72 cm; *, 5.08 cm; □, rectangular bed.

therefore, the condition for the tensile yield will be met first at the contact between the bed and the filter, or within the bed at the bottom (as predicted theoretically by Tsinontides and Jackson [4]), not at a higher level in the bed. In all cases studied, we observed that the filter surface remains covered by a thin layer of powder, and we conclude that toner-to-filter adhesion exceeds particle–particle cohesion, and so yield occurs in the powder at the bottom of the bed, and not at the powder–filter interface. The tensile strength of the powder is therefore given by:

$$\sigma_t = \Delta p - mg/A \qquad (3)$$

Other factors that need to be considered in setting up a powder bed measurement include the effect of filter uniformity and wall effects. Most of the work described in this paper has been done with a 5.07 cm diameter filter, and with bed heights from 0.5 to 5.0 cm, but we have also used filters of 4.09, 4.72 and 5.17 cm diameter, and also a filter of rectangular cross-section 3.35×7.5 cm^2. Results of tensile strength, σ_t, vs. consolidation stress, σ_c, shown in Fig. 7, for this range of experimental conditions, are the same within experimental error, and the fine filters give the same result, so neither filter non-uniformity nor wall effects are evident. This figure also shows the scatter to be expected in experiments of this type (error bars are omitted from later figures for the sake of clarity).

In these experiments, we have used a series of model xerographic toners, designed for us at Xerox. The series is designated RT-5462-2 (0.01% additive), RT-5114-3 (0.05% additive), RT-5115-2 (0.1% additive), RT-5116-2 (0.2% additive), and RT-5117-2 (0.4% additive). The series is based on one batch of polymer particles, so the only variable is the additive concentration. The toner polymer is styrene–butadiene with 2 wt.% cyan pigment, and the flow control additive is a fumed silica such as Aerosil® or Cab-o-sil® [10].[2] We have also tested Canon CLC-500 cyan toner. Particle diameter (volume average) in the RT series is 12.7 μm; the CLC-500 toner diameter (volume average) is 8.5 μm. The density of the toner particles for the RT series is $\rho_p = 1.965$ g/cm^3 while the density of the Canon CLC 500 toner additive is $\rho_p = 1.199$ g/cm^3, and that of the silica particle is $\rho_A = 2.2$ gr/cm^3. These density values were measured by using an AccuPyc 1330 Pycnometer.

[2] Aerosil is a tradename of Degussa, and Cab-o-sil is a tradename of Cabot.

3. Experimental results

Fine, cohesive powders do not pack uniformly under normal handling procedures, and this gives rise to erratic flow behavior. To overcome the problems associated with non-uniformity, our powder samples are initialized by being fluidized and then allowed to settle under gravity. As already noted, fluidization of the xerographic toners tested depends on the presence of the flow control additive; for toners with low additive concentration (0.01 to 0.05%) homogeneous fluidization is difficult to achieve and the sample is likely to rise in the bed as a plug that becomes unstable and then collapses. In order to achieve homogeneous fluidization of these samples, the powder bed is vibrated. For powders of lower cohesivity (greater additive concentration) plugs are rarely observed; after the break occurs, the fracture zone rises in the bed and then, at a certain height, the gas escapes from the powder through channels that erupt like miniature volcanoes. The lower the cohesivity, the less stable the channels. Finally, for the least cohesive powders (the RT5117 toner, with 0.4% additive, and the Cannon CLC-500 toner) plugs do not develop, channels are very unstable, and a state of homogeneous fluidization is readily achieved without the need for vibration. Thus, toners with low concentration of silica additive exhibit Type C behavior, while toners with high additive concentration exhibit Type A behavior. Clearly, therefore, interparticle cohesivity plays a dominant role in determining the fluidizability of fine powder, as pointed out by Molerus [11].

In Fig. 8 we show the trend of the average solid fraction with sample height at low consolidations for five model toners with additive concentration ranging from 0.01 to 0.4%. Powder layers were restricted to heights less than 5 cm to avoid any possible wall effect. In this figure, we see that all five powders follow the same general trend in behavior of the solid fraction with bed height (i.e., with consolidation stress), but the higher the additive concentration, the higher the value of solid fraction (i.e., lower value for void fraction, ε). This is a direct result of the lower particle cohesivity at higher additive concentration; the lower the cohesivity, the lower the friction, allowing the particles to slide over each other more easily, resulting in a tighter packing. Thus, there is a correlation between packing and flow: toners that flow well tend to pack well, and the reason behind this correlation is the cohesivity between particles.

The effect of additive concentration on void fraction is clearly seen in Fig. 9, where we present the average void

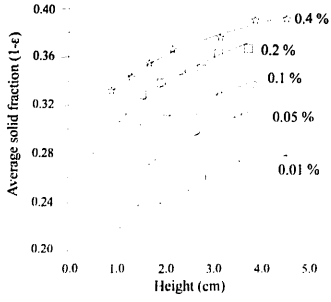

Fig. 8. Variation of average solid fraction $(1-\varepsilon)$ with height, for toners with different amounts of additive. Diameter of the bed 5.08 cm.

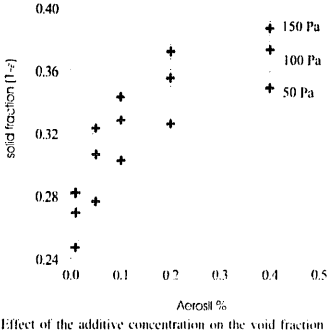

Fig. 9. Effect of the additive concentration on the void fraction for three different values of the powder mass.

fraction as a function of the additive concentration for three different values of the powder mass. We see that the effect of the additive on the void fraction is very pronounced for low concentrations, but the effect tends to saturate at concentrations greater than 0.4% (the reason for this saturation effect is discussed in Section 4.1). In Fig. 10, the consolidation stress is presented as a function of the height for the RT series of toners. Defining the compressibility as $\partial h/\partial\sigma_c$, the effect of the concentration of fumed silica on the compressibility is clearly seen. The slope of σ_c increases as a function of h as the additive concentration increases; this indicates that compressibility decreases slightly as additive concentration increases, because of the closer packing of the particles at higher additive concentrations.

In Fig. 11, the tensile stress at break (i.e., the tensile strength) is plotted against the height of the bed, and in Fig. 12, the tensile strength is plotted against the consolidation stress, σ_c. In both cases, we see an increase in the tensile strength with the degree of consolidation, and this implies plastic yield deformation of interparticle contacts; this will be discussed in Section 4. The difference in magnitude of

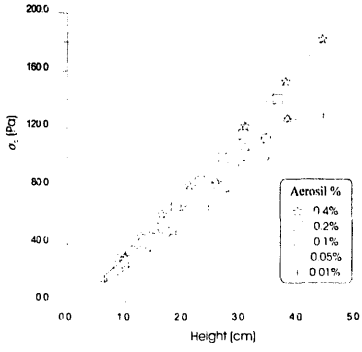

Fig. 10. Effect of the additive concentration on compressibility. Compressive stress as a function of the height for different concentrations of additive.

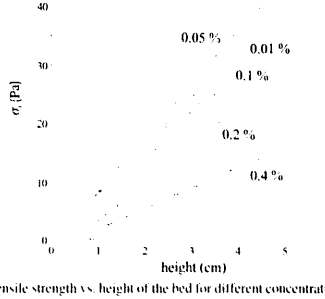

Fig. 11. Tensile strength vs. height of the bed for different concentrations of additive.

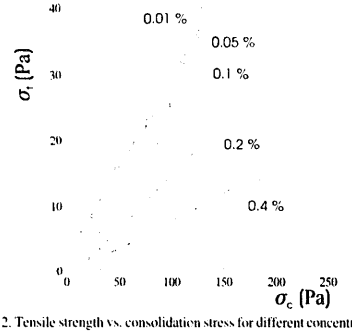

Fig. 12. Tensile strength vs. consolidation stress for different concentrations of additive.

tensile strength for a given consolidation stress varies according to the additive concentration; the lower the silica concen-

Table 1
Value of the slopes of F_t vs. F_c, for different additive concentrations

% Additive	F_t/F_c
0.01%	0.260 ± 0.020
0.05%	0.258 ± 0.007
0.1%	0.264 ± 0.017
0.2%	0.168 ± 0.003
0.4%	0.089 ± 0.005

tration, the higher the tensile strength; clearly the additive controls the tensile strength by controlling the cohesion between particles. Paying attention to the slope of the curves in Fig. 12, we notice that this slope is nearly the same for additive concentrations of 0.01, 0.05 and 0.1%, while the slope diminishes progressively for concentrations above 0.1%, consistent with the idea that at high additive concentrations, the interparticle contacts are harder (i.e., silica-dominated) than at low concentrations (Table 1).

A unifying concept, relating consolidation stress, tensile strength, and free volume, is the state diagram [2]. In this work, we have concentrated on the two-dimensional cross-section of the state diagram in the plane of zero shear, and in Fig. 13, our experimental results are presented in this form. The two families of curves in this figure are the consolidation stress loci and the tensile strength loci for zero shear stress as functions of the average void fraction, each line corresponding to a particular level of fumed silica additive. High concentrations of additive reduce the stress needed to cause a powder to flow, and the stress needed to consolidate it. Thus, at a constant value of consolidation stress, the porosity (i.e., the void fraction ε) has a lower value for a higher additive level, and this is a direct result of the increase in flowability, which increases the ability of the particles to rearrange themselves at a given stress level.

In the lower part of Fig. 13, the tensile strength of this family of powders is shown as a function of the void fraction, ε. For a given value of ε, the tensile strength decreases as the additive concentration increases. But as we have already noted, the compressive stress needed to achieve a given void

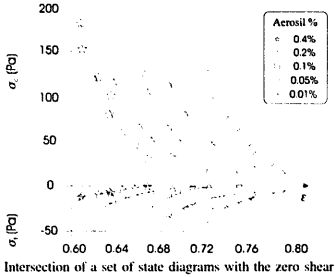

Fig. 13. Intersection of a set of state diagrams with the zero shear plane. Note that different concentrations of additive result in different state diagrams.

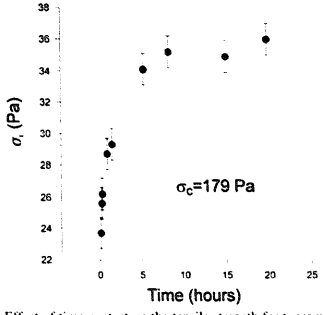

Fig. 14. Effect of time contact on the tensile strength for toner with 0.2% additive; consolidation stress σ_c = 179 Pa.

fraction is also related to the additive concentration. Thus, there is a complex relationship between consolidation stress, additive concentration, void fraction and tensile strength; the state diagram characterizes the relationships between these variables. We also note that for a constant value of consolidation stress (i.e., for the same toner mass in the powder bed) the tensile strength decreases with increasing additive concentration. This is directly related to the dependence of interparticle cohesion on the additive concentration. A further complication arises from the fact that the tensile strength increases as a function of the time of consolidation. For example, for the toner with 0.2% additive, we have found a 50% increase in tensile strength (but no measurable decrease in ε) for a waiting time of 8 h, after which time the affect saturates (see Fig. 14). This presumably indicates an increase in contact area with time due to plastic deformations of interparticle contacts. To avoid this complication, our measurements are taken within the first 5 min after the powder has been initialized.

4. The contacts between toner particles

One conclusion from our experimental work is that the interparticle forces in these cohesive powders, as measured by tensile strength, increase with consolidation stress, whereas for a system of elastic contacts, cohesive force should be independent of consolidation. This suggests that the interparticle contacts undergo plastic deformation even at very low consolidation stress. This observation is consistent with theory [12], in which the interparticle forces of adhesion at a contact can give rise to plastic deformation even at zero loads, for high surface energy materials. The next step in this work will be to proceed to higher consolidation stresses, and to look for a transition from plastic to elasto-plastic behavior, as predicted by theory. For the moment, however, we limit ourselves to estimating the magnitude of the interparticle forces for low consolidation stresses. To do this, we need a

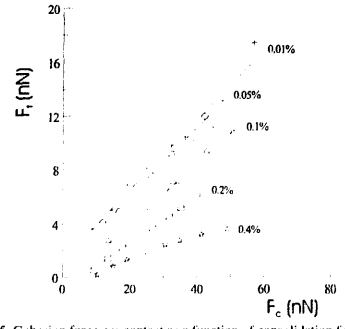

Fig. 15. Cohesion force per contact as a function of consolidation force per contact for different concentrations of additive.

relationship between the isotropic, normal stress, σ, and the contact force F; the simplest relationship of this type is for spherical particles with random packing, as defined by Rumpf [13].

$$\sigma \approx \frac{Fk(1-\varepsilon)}{d_p^2 \pi} \tag{4}$$

where d_p is the particle diameter, and k is the coordination number, i.e., the number of contacts per particle. A relationship between coordination number and ε was given by Jaraiz et al. [14], and from this we obtain the approximate formula,

$$k\varepsilon^{3/2} \approx \pi/2 \text{ for } \varepsilon > 0.6 \tag{5}$$

Using this relationship, we obtain

$$\sigma_c = \frac{(1-\varepsilon)F_c}{2\varepsilon^{3/2} d_p^2} \tag{6}$$

$$\sigma_t = \frac{(1-\varepsilon)F_t}{2\varepsilon^{3/2} d_p^2} \tag{7}$$

Obviously these relationships are only approximate as the toner particles are far from being spherical, and packing is not isotropic, but the equations provide us with a method for estimating the average consolidation force per contact, F_c, and the average cohesion force per contact, F_t. The results obtained for these microscopic forces are shown in Fig. 15 but it is important to realize that force will not be distributed uniformly through the contacts in the powder. It is well known that forces tend to be concentrated along force lines in a stressed, granular material [15], and as a consequence, local forces range widely about the average, but in the absence of more precise information, we can calculate the average values of force using Eqs. (6) and (7).

4.1. The distribution of surface additives

Typical S.E.M. micrographs of xerographic toner particles with surface additives are shown by Ott and Mizes [16]. From such micrographs, we observe that the additive particles are distributed in agglomerates with estimated diameters d_a from 40 to 60 nm. Since the individual silica particles have a diameter d_s of 7 nm, the number of particles per agglomerate should be approximately,

$$N_a = f\frac{d_a^3}{d_s^3} \approx 220 \pm 100 \tag{8}$$

where $f \sim 0.6$ is the solid fraction of the agglomerate (assuming random close packing). The change in interparticle contacts from polymer–silica to silica–silica should take place when the average distance between the centers of the agglomerates on the toner surface is twice the diameter of the agglomerate; for smaller spacing, the contact between polymer and silica is unlikely. In this case, the effective area covered by the agglomerate is around $(2d_a)^2$, and the number of agglomerates on the toner surface is

$$M_a = \pi \frac{d_p^2}{4d_a^2} \tag{9}$$

where d_p is the toner diameter. From this, we can estimate the percentage additive needed for the majority of contacts to be silica-to-silica:

$$x\% = 100 M_a N_a \frac{\rho_s d_a^3}{\rho_t d_p^3} = 100 f \frac{\pi}{4} \frac{\rho_s d_a}{\rho_t d_p} \approx 0.43\% \tag{10}$$

Where ρ_s and ρ_t are the densities of the fumed silica and the toner particles, respectively. Some factors may change this estimate; the toner area could be greater than that given by the average diameter, and the effective area covered by the agglomerate could be smaller in a closer packing. Nevertheless, the experimental saturation effect shown in Fig. 9 is around 0.5% additive, a value close to our estimate of 0.43%. We can also estimate the additive concentration corresponding to the change from polymer–polymer contacts to silica–polymer contacts. The average distance between silica agglomerates should be greater than a certain value to have the possibility of a toner-to-toner contact (see Fig. 16).

$$s^2 = 8R_t R_a + 4R_a^2 = 2d_t d_a + d_a^2 \approx 2d_t d_a \tag{11}$$

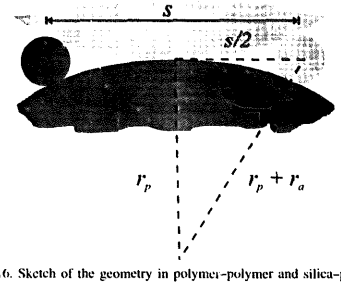

Fig. 16. Sketch of the geometry in polymer–polymer and silica–polymer contacts.

where R_1 is the local radius of curvature of the toner. If on average, adjacent Aerosil agglomerates belong to adjacent toner particles, the average distance between agglomerates on the same toner particle is $2s$, and the number of agglomerates on the toner surface should be,

$$M_a = \pi \frac{d_p^2}{4s^2} \quad (12)$$

The corresponding additive percentage should be

$$x\% = 100f \frac{\pi}{8} \frac{\rho_a d_a^2}{\rho_p d_1 d_p} \quad (13)$$

If we assume an average asperity diameter of 0.1 μm, the estimated value for this critical percentage is 0.1%. Obviously, these numbers are only rough estimates; nevertheless they support our hypothesis that in the range of additive concentrations from zero up to 0.1% the contacts change from polymer–polymer to polymer–silica and that, from 0.1 to 0.5% additive concentration the contacts change from polymer–silica to silica–silica. The silica has two effects: it increases the hardness of the contacts, and it reduces the size of the contact zone; both effects serve to reduce the interparticle cohesion.

5. Conclusions

We have developed a powder bed technique for the measurement of the state diagram of fine, cohesive powders under zero shear conditions. In these studies, we measure the free volume and tensile strength of the powder after it has been initialized, and then subjected to low levels of consolidation stress. We first obtain reproducible, stratified layers of consolidated powder by fluidizing the material, and then turning off the fluidizing gas, allowing the powder to settle; this technique enables us to obtain reproducibly initialized beds of powder, and from the relationship between height and mass in the bed, we calculate the packing fraction and free volume. The initialized powder is then subjected to an increasing negative tension by flowing gas through the bed until fracture occurs, and from this we obtain the tensile strength of the powder corresponding to a given value of consolidation stress, and hence of free volume, i.e., void fraction.

Measurements have been made of void fraction and tensile strength vs. consolidation stress for a set of model xerographic toners with a range of flow control additives such as Aerosil® and Cab-o-sil®. From these measurements, we have constructed the corresponding state diagrams, showing the relationships between σ_c, σ_t and ε, at zero shear stress. From the conditions for fluidization, we find that for fine particles, the boundary between hard-to-fluidize powders, and easily fluidized powders depends strongly on the interparticle cohesivity. The cohesivity of the 12.7 μm polymer particles (which cannot be fluidized) can be reduced by an order of magnitude by blending with a fumed silica additive, and thus the base material can be transformed into a readily fluidized powder. The most cohesive toner that can be fluidized (by the simultaneous application of gas flow and vibration) contains 0.01% additive by weight. The interparticle forces corresponding to this additive concentration extrapolates to 2 nN at zero consolidation, and rises linearly to 14 nN at 50 nN consolidation force; for comparison, the gravitational force on an individual particle is about 0.01 nN. For this reason, when the particles settle into their initialized state after fluidization, cohesive forces dominate, and the particles condense into a very open structure that approaches the ballistic aggregation limit [7]. From Fig. 8, the average solid fraction, $(1-\varepsilon)$ for the toner with 0.01% additive extrapolates to about 0.16 at zero consolidation stress; that is to be compared with the random ballistic deposition limit of 0.15.

Finally, we note that at the low compressive stresses we have examined, tensile strength is linearly related to consolidation stress, and this indicates that the contacts are fully plastic under these conditions. Our next step will be to investigate higher consolidation stresses in the expectation that a transition from plastic to elasto-plastic behavior will be observed.

Acknowledgements

We are indebted to Alberto Pérez for his work in this area, to Mike Morgan and Frank Genovese for their help, and to Paul Julien for providing us the toners used in this study. This research has been supported by the Xerox Foundation, Xerox and by the Spanish Government Agency Dirección General Co. de Cincia y Tecenología (DGCYT) under Contract PB96-1375.

References

[1] K. Rietema, The Dynamics of Fine Powders, Elsevier, UK, 1991.
[2] O. Molerus, Powder Technol. 12 (1975) 259.
[3] D. Geldart, Powder Technol. 7 (1973) 285.
[4] S.C. Tsinontides, R. Jackson, J. Fluid Mech. 255 (1993) 237.
[5] H.O. Kono, Y. Itami, E. Aksoy, AIChE Symp. Ser. 90 (301) (1994) 45.
[6] J.P.K. Seville, R. Clift, Powder Technol. 37 (1984) 117.
[7] P.K. Watson, H.A. Mizes, A. Castellanos, A. Pérez, in: Behringer, Jenkins (Eds.), Powders and Grains 97, Balkema, Rotterdam, 1997, p. 109.
[8] E. Marring, A.C. Hoffman, L. Janssen, Powder Technol. 79 (1994) 1.
[9] R.M. Nedderman, Statics and Kinematics of Granular Materials, Cambridge, 1992.
[10] D. Barby, in: Parfitt, Sing (Eds.), Characterization of Powder Surfaces, Chap. 8, Academic Press, 1976.
[11] O. Molerus, Powder Technol. 33 (1982) 81.
[12] D. Maugis, H.M. Pollock, Acta Metall. 32 (1984) 1323.
[13] H. Rumpf, Chem. Ing. Tech. 30 (3) (1958) 144.
[14] E. Jaraiz, S. Kimura, O. Levenspiel, Powder Technol. 72 (1992) 23.
[15] C.H. Liu, et al., Science 269 (1995) 513.
[16] M.L. Ott, H.A. Mizes, Colloids Surf. A 87 (1994) 245.